Energy Calibration of High-Resolution X-Ray TES Microcalorimeters With 3 eV Optical Photons

F. T. Jaeckel, C. V. Ambarish, N. Christensen, R. Gruenke, L. Hu, D. McCammon, M. McPheron, M. Meyer, K. L. Nelms, A. Roy, D. Wulf, S. Zhang, Y. Zhou, J. S. Adams, S. R. Bandler, J. A. Chervenak, A. M. Datesman, M. E. Eckart, A. J. Ewin, F. M. Finkbeiner, R. Kelley, C. A. Kilbourne, A. R. Miniussi, F. S. Porter, J. E. Sadleir, K. Sakai, S. J. Smith, N. Wakeham, E. Wassell, W. Yoon, K. M. Morgan, D. R. Schmidt, D. S. Swetz, and J. N. Ullom

***Abstract*—With the improving energy resolution of transition-edge sensor (TES) based microcalorimeters, performance verification and calibration of these detectors have become increasingly challenging, especially in the energy range below 1 keV where fluorescent atomic X-ray lines have linewidths that are wider than the detector energy resolution and require impractically high statistics to determine the gain and deconvolve the instrumental profile. Better behaved calibration sources such as grating monochromators are too cumbersome for space missions and are difficult to use in the lab. As an alternative, we are exploring the use of pulses of 3 eV optical photons delivered by an optical fiber to generate combs of known energies with known arrival times. Here, we discuss initial results of this technique obtained with 2 and 0.7 eV resolution X-ray microcalorimeters. With the 2 eV detector, we have achieved photon number resolution for pulses with mean photon number up to 133 (corresponding to 0.4 keV).**

***Index Terms*—Calibration sources, Energy resolution, Microcalorimeters, Transition edge sensors, X-ray detectors.**

I. Introduction

IT IS now accepted that most of the normal matter in our Universe resides in diffuse structures at temperatures near 10^6 K and above [1]. At these temperatures matter is primarily observable only in X-rays, and instrumental limitations result in our current situation where the distribution and state of this material is poorly understood and much of it is undetected entirely.

The instrumental difficulties involved with understanding the diffuse X-ray background are several: observing diffuse emission requires fast optics and a large field of view, which are difficult to achieve at X-ray wavelengths. Most of the gas is at temperatures near 10^6 K, resulting in most of the emission concentrated in lines below 600 eV. Existing X-ray observatories have poor efficiency at these energies, and energy resolutions of better than about 2 eV are required to resolve the dense forest of atomic lines in this energy range. These lines, their linewidths, and associated line-ratios with higher-charged species are a valuable diagnostic tool for understanding temperature and density evolution of diffuse interstellar gas in our universe. These requirements can realistically only be satisfied by X-ray microcalorimeters. Transition edge sensors have in principle demonstrated the required energy resolution and can be assembled in arrays of useful sizes to provide the necessary collection area on a sounding rocket or satellite mission [2].

However, because the detector gain is sensitive to environmental (and time varying) parameters such as operating temperature, radiative loading, and magnetic fields, these detectors require continuous tracking of gain drifts. They can also be quite non-linear, so for accurate determination of energies the use of several calibration lines is essential. While for ground-based characterization and calibration narrow line X-ray sources such as X-ray monochromators, electron-beam ion-traps, or synchrotron radiation can be used, these sources are cumbersome even in a laboratory environment and not practical for space missions because of their size and weight. The X-ray K_α fluorescence lines below 400 eV are several eV wide, much larger than the targeted detector resolution. Moreover, their profiles are not well known and can be subject to chemical shifts. In conclusion, there is currently no satisfactory way to determine detector energy resolution or obtain gain calibration in the energy range of interest.

However, as has been proposed in reference [3], X-ray calibration events could be simulated by delivering pulses of optical photons with known energy. Additional advantages would include the ability to have any desired timing and cover any desired energy range that one wishes to calibrate for. There will be Poisson fluctuations in the number of photons striking a pixel in a given pulse, resulting in a series of lines spaced at the optical photon energy. The detector energy resolution must be better than this spacing for this technique to be useful. The photon energy must also be low enough to avoid any photo-electron

Manuscript received November 12, 2018; accepted February 9, 2019. Date of publication February 18, 2019; date of current version March 18, 2019. This work was supported by NASA under Grant NNX16AM31G. *(Corresponding author: Felix Till Jaeckel.)*

F. T. Jaeckel, C. V. Ambarish, N. Christensen, R. Gruenke, L. Hu, D. McCammon, M. McPheron, M. Meyer, K. L. Nelms, A. Roy, D. Wulf, S. Zhang, and Y. Zhou are with the Department of Physics, University of Wisconsin-Madison, Madison, WI 53706 USA (e-mail: felix.jaeckel@wisc.edu).

J. S. Adams, S. R. Bandler, J. A. Chervenak, A. M. Datesman, M. E. Eckart, A. J. Ewin, F. M. Finkbeiner, R. Kelley, C. A. Kilbourne, A. R. Miniussi, F. S. Porter, J. E. Sadleir, K. Sakai, S. J. Smith, N. Wakeham, E. Wassell, and W. Yoon are with the NASA Goddard Space Flight Center, Greenbelt, MD 20771 USA.

K. M. Morgan and J. N. Ullom are with the National Institute for Standards and Technology, Boulder, CO 80305 USA, and also with the University of Colorado, Boulder, Boulder CO 80309 USA.

D. R. Schmidt and D. S. Swetz are with the National Institute for Standards and Technology, Boulder, CO 80305 USA.

Color versions of one or more of the figures in this paper are available online at http://ieeexplore.ieee.org.

Digital Object Identifier 10.1109/TASC.2019.2899856

emission from the absorber, since this would cause loss of some fraction of the photon's energy. The maximum energy where most materials have zero photoelectric efficiency is about 3 eV, so detectors with energy resolution better than 2 eV FWHM are required. The ready availability of 'blu-ray' laser diodes at 3.06 eV is convenient.

While photon number resolution has already been demonstrated [3], [4], the energy spectra showed a quick degradation in energy resolution even for around 10 photons. Although detailed spectral fits were not provided in these papers, the spectra shown are roughly consistent with an energy loss of between 0.8 eV and 1.4 eV occurring for some non-negligible fraction of the detected photons, leading to a filling in of the valleys and ultimately to the loss of photon number resolving ability. Equivalently, one could also assume that additional energy of between 1.6 and 2.2 eV was delivered for a fraction of the photons, e.g. due to fluorescence of the fiber or other stimulated emission. The promises and limitations of these previous results drive us to attempt this again to see if this technique could be viable and to make progress on understanding the cause of the low energy tail. Following a brief overview of the experimental setup (similar to the one described in reference [3]), we will discuss results obtained with two different TES detector chips selected for this purpose.

II. Experimental Setup

The detector chips are housed inside a light-tight and magnetically shielded box on the FAA stage of a standard two-stage adiabatic demagnetization refrigerator (ADR). Detectors are read-out by a two-stage superconducting quantum interference device (SQUID) read-out [5], consisting of 10 nH input inductance first stage SQUID with built-in 250 $\mu\Omega$ shunt resistors, followed by 2nd stage SQUID array amplifiers on the 3 K stage of the cryostat. A field coil inside the TES test box allows us to cancel residual fields.

A. Laser Diode

A standard blu-ray UV laser diode heat sunk to a block of copper was used for our experiments. The laser diode has a linewidth of about 1 nm around 405 nm as verified by an optical grating spectrometer. This translates into a FWHM of 7.5 meV for a single photon. For a pulse of n photons, the linewidth should scale as $\sqrt{n}$, so we expect a FWHM of 0.075 eV for a 100 photon, 306 eV calibration pulse. Temperature and current induced wavelength shift have been measured and reported in reference [3] and are small enough to not be of concern for the measurements presented here. A multimode fiber was glued to the front of the diode case with Stycast 1266. As shown in Fig. 1, the fiber is then routed into the cryostat through a commercial vacuum hermetic feedthrough [6]. At the 3K stage, a filter consisting of a hot mirror and KG-5 Schott filter glass (both Edmund Optics) rejects infrared radiation above 750 nm and also attenuates the incoming light by 3 orders of magnitude due the free space geometry without coupling lenses. Additional attenuation is added on the outside as needed with neutral density filters. Optionally, a monochromator can be inserted into the light path. The fiber enters the TES box through a small penetration in the shields and the light from the bare cleaved end illuminates the central region of the detector chip from a distance of a few millimeters. The laser diode is driven with 20 ns to 1 μs current pulses at about 30% above the lasing threshold.

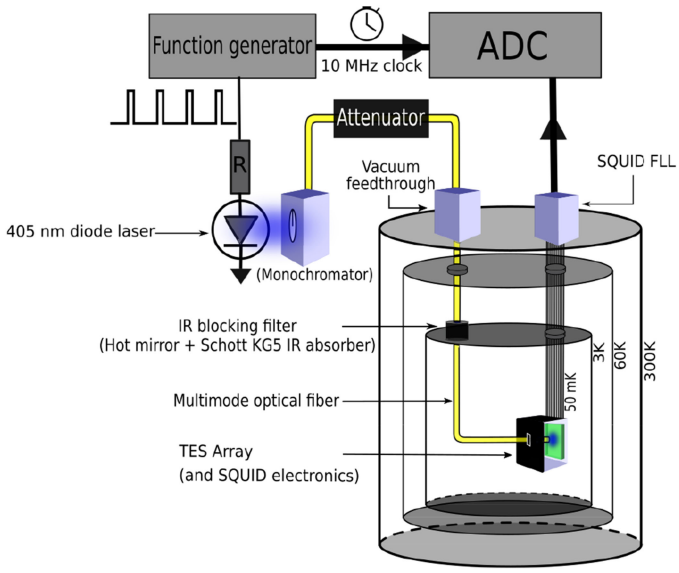

Fig. 1. Light path setup inside the cryostat.

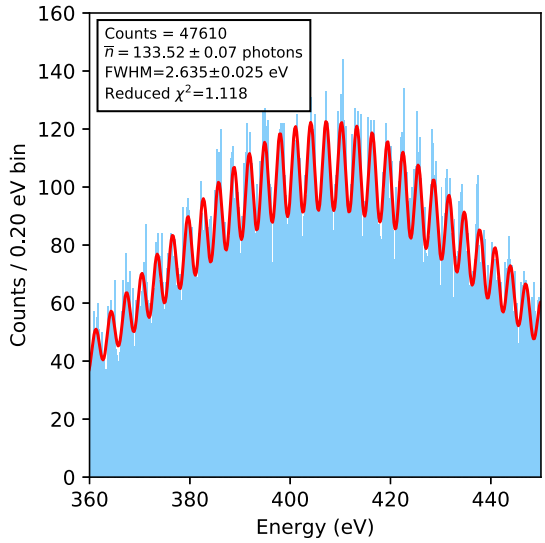

Fig. 2. Spectrum obtained on the large absorber TES chip for pulses with mean photon number $\bar{n} = 133$.

B. Large Absorber TES Detector Chip

The first detector chip used for these tests was a 8 × 8 array of 120 μm × 120 μm Mo/Au TES ($T_c \approx 85$ mK) with 240 μm square absorbers made from 1.5 μm gold and 3 μm electroplated bismuth. The array was fabricated at Goddard Space Flight Center and had achieved energy resolution of around 2.3 eV for 6 keV photons. Devices with 0% and 75% membrane perforations were used for this test, although only results for the 0% perforation device are shown.

The pulse height spectrum obtained with $\bar{n} = 133$ is shown in Fig. 2. For analysis, we have made use of an optimal matched

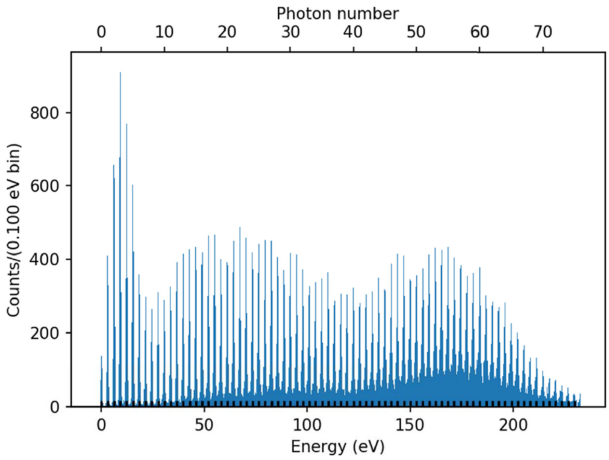

Fig. 3. Pulse height spectrum obtained on the high resolution NIST TES detector using a range of laser pulse widths to provide overlapped distributions covering the energy range shown.

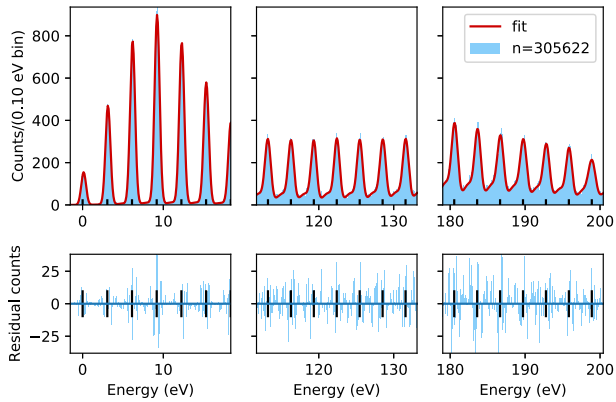

Fig. 4. Three expanded sections of a two-Gaussian fit to the spectrum in Fig. 3. The ratio of the area of the second Gaussian to that of the main peak was assumed to be proportional to the number of photons in the main peak, as expected for a fixed fraction of the photons having a fixed energy deficit. See text for best fit parameters.

filter and the overlapped pulse fitting technique reported in reference [7]. Portions of the pulse height spectra from the laser pulses can be resolved. This is an improvement over the result of previous experiments that demonstrates that the proposed concept is usable for detector calibration. The fit lines shown in red are Gaussian fits to the peaks to determine energy resolution. The baseline energy resolution of around 1.8 eV degrades more quickly than expected for these devices to about 2.6 eV at 400 eV. Part of this degradation might be due to valleys filling in for higher photon numbers as had been observed in previous experiments on other detectors. However, since the tops of the peaks also appear to be getting wider, the dominant mechanism here may well be due to gain variations or extra noise due to laser power incident on the entire chip. Overall the energy resolution of this detector was not good enough to warrant more detailed fits.

III. High Resolution TES Spectra

For a more detailed investigation of the cause of degradation in energy resolution, we used a high resolution detector chip fabricated at NIST. These devices have a 3.4 μm layer bismuth absorber evaporated directly on top of the 120 μm $\times$ 120 μm TES ($T_c \approx 75$ mK). A gold coated Si collimator chip with 60 μm $\times$ 60 μm deep-reactive-ion etched apertures was aligned and mounted on top of the TES to reduce the number of stray photons impinging on the TES chip. Both detector and aperture chips were separately heat sunk to the copper cold stage with gold wire bonds.

To account for the non-linearity of the detector, optimum filtered pulse heights were converted into energy via a quadratic polynomial, whose coefficients were determined by fitting expected photon pulse energy $n \cdot E_0$ against corresponding peak centroids of the pulse-height histogram. The magnitude of the non-linear term for this dataset is about 19.6 eV at 235.6 eV ($n = 77$). The entire spectrum is show in Fig. 3 and contains over 300,000 pulses taken at several different $\bar{n}$ values. The baseline resolution for this detector was about 0.71 eV. At low energies, we note the near absence of counts between the integer photon number peaks. Towards higher energies, the space around the ½ integers begins to fill in.

To analyze the spectra quantitatively, two models were then considered: a) Gaussian with low energy bump, and b) low energy exponential tails.

A. Gaussian With Low Energy Bump

This model was motivated by the low energy bump clearly resolved in the earlier experiments [4]. The TES energy-response was modelled as a Gaussian. A second Gaussian with lower energy and relative intensity proportional to the number of photons in the main peak was added to account for a certain probability for a photon to have its energy shifted by a fixed amount. The bump energy shift was allowed to vary between 0.2 and 1.5 eV and additional broadening was allowed for the bump. The best fit shown in Fig. 4 has a bump energy shift of 1.2 eV and a FWHM of 1.502 eV with a probability of 0.91%. The fit has a reduced χ^2 of 1.3. A systematic discrepancy between the fit and data is clearly apparent from the residuals in the mid-energy range.

B. Bortels Function

Non-Gaussian low energy tails have been observed in the spectra of TESs with evaporated bismuth absorbers [8]. The tail has typically been modelled with a Bortels function [9], which is the convolution of a sum of the exponential tail and a delta function with a Gaussian. The relative contribution of tail compared to the central Gaussian peak has been found to grow with the photon energy [10]. We assumed the relative amplitude of the tail to be proportional to the main peak energy. The proportionality constant and the exponential energy decay scale of the tail were free parameters.

The best fit for this model (reduced χ^2 of 1.3) is shown in Fig. 5. The tail exponential energy decay scale comes out to be 1.95 eV with an amplitude proportionality constant of about 0.39%.

The degradation of the FWHM of the Gaussian component is shown in Fig. 6. Again, this degradation is larger than would be

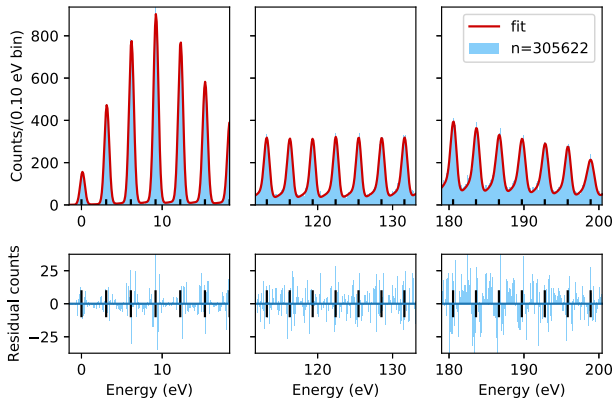

Fig. 5. Fit to spectrum of Fig. 3 using a one-sided exponential tail function. See text for best-fit parameters.

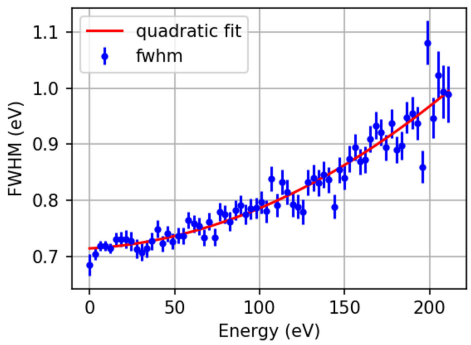

Fig. 6. Variation of FWHM of fitted pulses with photon energy. Quadratic fit (red-line) is a guide for the eye.

expected for these detectors and is at least partially attributable to uncorrected drifts in the detector gain.

C. Laser Spectrum and Monochromator for Narrow Line-Width

While the 1 nm linewidth of the bare laser diode is sufficient for the ∼300 eV calibration range required for a soft X-ray sounding rocket mission, it is worthwhile pursuing even narrower line width for applications that require a calibration source at higher photon energies.

We are exploring the use of a monochromator to further reduce the laser line width. We have set up a simple Fastie-Ebert grating monochromator, consisting primarily of a 150 mm focal length concave mirror, a 3600 lines/mm holographic grating in Littrow configuration, and a set of entrance and exit slits. The laser diode was found to operate over about eight cavity modes with a spacing of about 70 pm. Because the mode distribution shifts with laser operating conditions (temperature, current), it is convenient to make the exit slit of the monochromator just slightly wider than that of the line spacing so that at least one mode is always transmitted. This would result in an energy resolution of about 0.6 meV for a single photon, or just 27 meV for a simulated 6 keV photon. An alternative approach, the stabilization of the laser emission wavelength by an external cavity formed by a grating, was also considered. While this approach allows optical line width down into the kHz range, it places stringent requirements on temperature and mechanical stability. It is also not clear that this would work under pulsed conditions.

IV. Conclusion

We have demonstrated that 405 nm photon pulses can be resolved with TES X-ray microcalorimeters out to photon numbers of at least 130 (or 400 eV), thus providing a convenient source for laboratory performance verification and in-flight calibration of detectors for a low-energy X-ray sounding rocket or satellite mission. The degradation with increasing photon number is much smaller than in previous experiments, showing that this does not present an insurmountable problem for calibration at low energies. Further improvements are likely once the causes of the current fill-in and broadening are better understood. Possible degradation mechanisms under investigation include unwanted lower-energy photons from fluorescence processes in the setup, pulse-to-pulse variations in thermal cross-talk from fluctuations in optical loading, or energy losses via photoelectric effect or meta-stable states (e.g. in the absorber). The experimental configuration (i.e. illumination, geometry, and device construction) is expected to affect the relative significance of these processes. Hence, the improvement over previous results may be attributable to differences in the setup. Further experiments will be required to discern the underlying issues. Whether or not we can eventually get above 6 keV (>2000 photons) remains to be seen.

Acknowledgment

The authors would like to thank Jim Lawler, Mark Saffman, Deniz Yavuz, Jim Reardon, and Brett Unks from the Department of Physics, UW Madison, for their assistance with some aspects of the optical setup.

References

[1] K. Nandra *et al.*, "The hot and energetic universe: A white paper presenting the science theme motivating the Athena+ mission," 2013, arXiv:1306.2307 [astro-ph.HE].
[2] K. Morgan, S. Busch, M. Eckart, C. Kilbourne, and D. McCammon, "Large area transition edge sensor X-ray microcalorimeters for diffuse X-ray background studies," *J. Low Temp. Phys.*, vol. 176, no. 3/4, pp. 331–336, 2014.
[3] M. Hokin *et al.*, "Narrow line X-ray calibration source for high resolution microcalorimeters," *J. Low Temp. Phys.*, vol. 176, no. 3/4, pp. 566–570, 2014.
[4] D. J. Fixsen, S. Moseley, T. Gerrits, A. E. Lita, and S. W. Nam, "Optimal energy measurement in nonlinear systems: An application of differential geometry," *J. Low Temp. Phys.*, vol. 176, no. 1/2, pp. 16–26, 2014.
[5] STAR Cryoelectronics, Santa Fe, NM, USA, 2016. [Online]. Available: http://www.starcryo.com/
[6] OZ Optics, Toronto, ON, Canada, 2015. [Online]. Available: http://www.ozoptics.com/
[7] D. Wulf, F. Jaeckel, D. McCammon, and K. M. Morgan, "Technique for recovering pile-up events from microcalorimeter data," *J. Low Temp. Phys.*, vol. 184, pp. 431–435, Jul. 2016.
[8] D. Yan *et al.*, "Eliminating the non-Gaussian spectral response of X-ray absorbers for transition-edge sensors," *Appl. Phys. Lett.*, vol. 111, no. 19, 2017, Art. no. 192602.
[9] G. Bortels and P. Collaers, "Analytical function for fitting peaks in alpha-particle spectra from Si detectors," *Int. J. Radiat. Appl. Instrum. Part A. Appl. Radiat. Isot.*, vol. 38, no. 10, pp. 831–837, 1987.
[10] J. Fowler *et al.*, "A reassessment of absolute energies of the X-ray L lines of lanthanide metals," *Metrologia*, vol. 54, no. 4, pp. 494–511, 2017.